

Technical University of Denmark



## The Multi-Detector Powder Neutron Diffractometer at Risø National Laboratory

Als-Nielsen, Jens Aage; Andersen, Niels Hessel; Broholm, C.; Clausen, K.N.; Lebech, Bente

*Publication date:*  
1988

*Document Version*  
Publisher's PDF, also known as Version of record

[Link back to DTU Orbit](#)

*Citation (APA):*  
Als-Nielsen, J. A., Andersen, N. H., Broholm, C., Clausen, K. N., & Lebech, B. (1988). The Multi-Detector Powder Neutron Diffractometer at Risø National Laboratory. (Risø-M; No. 2720).

### DTU Library

Technical Information Center of Denmark

---

#### General rights

Copyright and moral rights for the publications made accessible in the public portal are retained by the authors and/or other copyright owners and it is a condition of accessing publications that users recognise and abide by the legal requirements associated with these rights.

- Users may download and print one copy of any publication from the public portal for the purpose of private study or research.
- You may not further distribute the material or use it for any profit-making activity or commercial gain
- You may freely distribute the URL identifying the publication in the public portal

If you believe that this document breaches copyright please contact us providing details, and we will remove access to the work immediately and investigate your claim.

# **The Multi-Detector Powder Neutron Diffractometer at Risø National Laboratory**

**J. Als-Nielsen, N. H. Andersen, C. Broholm, K.N. Clausen and  
B. Lebech**

**Abstract.** The report describes a new multi-detector powder neutron diffractometer installed at the DR3 reactor at Risø. The report gives details of the design criteria and operating instructions in order to ease operation of the instrument by actual and potential users. The individual components (collimators, monochromator, detectors) are described in detail. An example of a study of the oxygen uptake of  $\text{YBa}_2\text{Cu}_3\text{O}_{7-x}$  is given.

**Risø National Laboratory, DK-4000 Roskilde, Denmark  
June 1988**

**ISBN 87-550-1434-8**  
**ISSN 0418-6435**  
**Grafisk Service, Risø**

# Contents

	Page
<b>1. Introduction</b> .....	5
1.1. Principles of Powder Diffraction .....	5
1.2. Design Criteria .....	7
<b>2. Monochromator</b> .....	9
2.1. Lattice Spacing .....	9
2.2. Higher Order Contamination .....	9
2.3. Mosaicity .....	10
2.4. Sagital Focussing .....	10
<b>3. Collimators</b> .....	10
<b>4. Detectors and Electronics</b> .....	12
<b>5. Powder Spectrum Resolution</b> .....	12
<b>6. Software</b> .....	14
6.1. Single Detector Mode .....	14
6.2. Multi Detector Mode .....	15
<b>7. Lining-up the Multi-Detector Diffractometer</b> .....	16
7.1. Monochromator .....	17
7.2. Monochromator-Sample Collimator .....	17
7.3. Sample Table Alignment .....	17
7.4. Sample Scattering Angle .....	18
7.5. Detector-Bank Collimator Alignment .....	18
7.6. Monochromator Scattering Angle .....	18
<b>8. Example of a Structure Study</b> .....	18
8.1. Phase Equilibrium and Kinetics of the Uptake of Oxygen of $\text{YBa}_2\text{Cu}_3\text{O}_{7-x}$ .....	19
<b>Acknowledgements</b> .....	21
<b>9. Appendices</b>	
A1. Summary Sheet for the Risø Powder Diffractometer ..	23
A2. Electronic Set-Up .....	25
A3. Powder Line-Broadening due to Vertical Divergence ..	27
A4. Example of Computer Aided Line-Up Sequence .....	31



# 1. Introduction

## 1.1. Principles of Powder Diffraction

The principles of diffraction of X-rays from a crystalline powder has been known for more than 75 years. The diffraction pattern yields detailed information about the atomic structure of crystalline material. The same principles apply for neutron beams as demonstrated in the pioneering experiments about 40 years ago. However, neutron diffraction has some special features: Light atoms or isotopes thereof diffract as well as heavier atoms and it is often possible to locate the position in the unit cell of e.g. hydrogen (deuterium) or oxygen atoms from a neutron powder diffraction pattern. Because of the magnetic moment of the neutron one can determine *magnetic* structures from neutron powder patterns. Neutron beams are very penetrating and the sample can therefore be placed in furnaces, magnets and/or suitable sample containers.

The method of powder diffraction is a mature field and the reader should not expect to learn about some *new* fundamental principles from this report; the basic techniques are described in standard textbooks on diffraction and crystal structure analysis (e.g. G.E. Bacon, "Neutron Diffraction" (Clarendon Press, Oxford) 1975). Here it suffices to

recapitulate that one obtains two kinds of information from a diffraction pattern:

- (i) From the *location* of the peaks in the spectrum one gets the dimensions of the unit cell, which in turn may be used to identify the chemical compound(s) in the sample and possibly contaminating phases.
- (ii) From the peak *intensities* one can derive the coordinates of the atoms within the unit cell as well as the thermal vibration amplitudes and site occupancies.

In this report we describe a new neutron powder diffractometer, which has been installed at the DR3 reactor at Risø, in order to ease the operation of this instrument by actual and potential users. Let us start by recapitulating the salient features of neutron powder diffraction. A monochromatic neutron beam is extracted from the Maxwellian spectrum emerging from the reactor by Bragg reflection from a single crystal, c.f. Fig. 1. The wave vector  $k$  of the monochromatic beam is related to the Bragg angle  $\theta_M$  and the reciprocal lattice vector of the monochromator  $\iota_M$

$$2k \sin \theta_M = \iota_M \quad (1)$$

The monochromatic beam is Bragg reflected from crystalline grains in the powder sample into Debye-Scherrer cones. The scattering angle of a particular cone,  $2\theta_S = 2\theta_{hkl}$  is related to the reciprocal lattice vector  $\iota_{hkl}$  by

$$2k \sin \theta_{hkl} = \iota_{hkl} \quad (2)$$

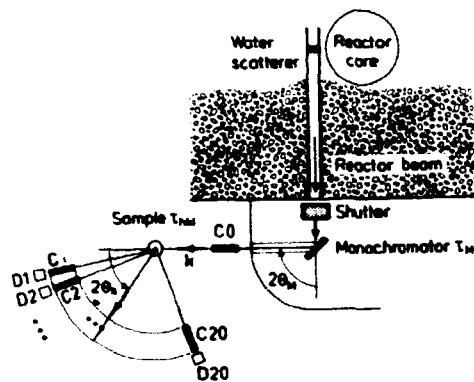


Fig. 1. Layout of the multi-detector powder diffractometer at DR3, Risø. Twenty detectors D1...D20 with Soller collimators C1...C20 spans 100° of scattering angle so a 5° scan of the detector bank furnishes the complete powder pattern. CO defines the collimation of the incident beam.

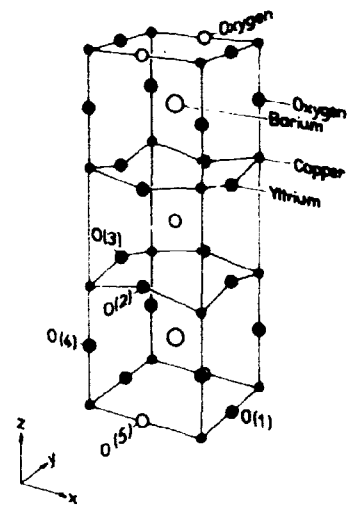


Fig. 2. Unit cell of  $YBa_2Cu_3O_{7-x}$ . Site O(5) is not occupied for  $x = 0$  (see section 8.1).

The reciprocal lattice vector  $\mathbf{r}_{hkl}$  has integer coordinates  $(h, k, \ell)$ , the so-called Miller indices. The unit cell in reciprocal space is spanned by  $(h, k, \ell) = (1, 0, 0)$ ,  $(0, 1, 0)$  and  $(0, 0, 1)$  and these basis vectors are denoted  $\mathbf{a}^*$ ,  $\mathbf{b}^*$  and  $\mathbf{c}^*$ , respectively. They are related to the real space unit cell basis vectors  $\mathbf{a}$ ,  $\mathbf{b}$ , and  $\mathbf{c}$  by

$$\begin{aligned} \mathbf{a}^*/2\pi &= \mathbf{b} \times \mathbf{c} / V, \\ \mathbf{b}^*/2\pi &= \mathbf{c} \times \mathbf{a} / V, \quad \mathbf{c}^*/2\pi = \mathbf{a} \times \mathbf{b} / V, \end{aligned}$$

with

$$V = (\mathbf{a} \times \mathbf{b}) \cdot \mathbf{c}$$

The amplitude of the  $(h, k, \ell)$  Bragg scattered wave is proportional to the structure factor  $F_{hkl}$

$$F_{hkl} = \sum_j f_j \exp(i\mathbf{r}_{hkl} \cdot \mathbf{r}_j) \quad (4)$$

In Eq. (3)  $\mathbf{r}_j$  denotes the position of the  $j$ 'th atom in the unit cell. An example of a unit cell is given in Fig. 2. The  $j$ 'th atom (or for neutron scattering rather the  $j$ 'th nucleus) has a scattering length  $b_j$ , an average site occupancy  $c_j$  and a mean squared thermal vibration amplitude  $\langle u_j^2 \rangle$ . The quantity  $f_j$  in Eq. (3) is defined as

$$f_j = c_j b_j \exp(-\mathbf{r}_{hkl}^2 \langle u_j^2 \rangle) \quad (4)$$

The intensity  $I_{hkl}$  integrated over scattering angle is proportional to the square of the structure factor

$$I_{hkl} \propto j_{hkl} L(\theta_{hkl}) |F_{hkl}|^2 \quad (5)$$

Here  $j_{hkl}$  is the multiplicity of the  $(h, k, \ell)$  reflection and  $L(\theta_{hkl})$ , the Lorentz factor, is a smooth and well known function of the scattering angle  $\theta_{hkl}$ .

## 1.2. Design Criteria

A powder spectrum obtained with the new diffractometer is shown in Fig. 3. It contains about 50 separated powder peaks at positions corresponding to a range of  $\nu_{hkl}$  moduli from  $1.5 \text{ \AA}^{-1}$  to  $8 \text{ \AA}^{-1}$ . The line spacing decreases with increasing angle simply because the density of moduli  $\nu_{hkl}$  increases with increasing Miller indices. The variation of peak intensities reflects the variation of the structure factor, c.f. Eqs. (3) and (5), with  $(h,k,\ell)$ . The observable dynamic range of intensities is about 100:1. This range is determined by the background level which in turn is given by the sum of a general stray neutron background level and the diffuse scattering from the sample and sample container. The latter contribution is the dominant part in Fig. 3.

The quantities one wants to obtain from a powder diffraction measurement are the atomic positions  $r_j$  in the unit cell as well as the site occupancy  $c_j$  and the root mean square (r.m.s.) thermal amplitude  $\langle u_j^2 \rangle^{1/2}$ . Usually this is obtained by *modelling* the unit cell with a certain number of adjustable parameters, calculating the structure factor by Eqs. (3) and (4) and comparing to the measured intensities using Eq. (5). The number of measured reflections thus determines the maximum number of adjustable parameters in the model unit cell.

We shall now discuss the means to obtain the maximal number of reflections within a reasonably short time. First of all we note in conjunction with Eq.(2) that only grains with the correct orientation contribute to an  $(h,k,\ell)$  reflection. The correct orientation means that the reciprocal lattice vector of the reflecting grain is at an angle of  $\pi/2 - \theta_{hkl}$  with respect to the incoming beam direction. Second, only a relatively small part of the Debye-Scherrer cone is subtended by the detector. Therefore the intensity, even at a scattering angle where the Bragg law of Eq. (2) is fulfilled, is rather low – certainly less than 0.1% of the incident beam intensity, so a counting time of say at least ten seconds is needed to obtain sufficient accuracy. Furthermore, the Bragg peaks are progressively more closely spaced as one moves to higher and higher  $(h,k,\ell)$  indices, i.e. to larger scattering angle. So in order to separate the Bragg peaks the resolution must be narrow at large scattering angles. As will be explained in section 5, the high angle resolution is proportional to the inverse of  $\tan(\theta_M)$ . It is therefore advantageous to operate at a rather large value of  $\theta_M$ .

The required resolution implies also that the incident as well as the scattered beams must be well collimated, a condition which can only be obtained at the expense of intensity. So how can one compensate for the inherent low intensity? First of all one does not need a high angular resolution perpendicular to the



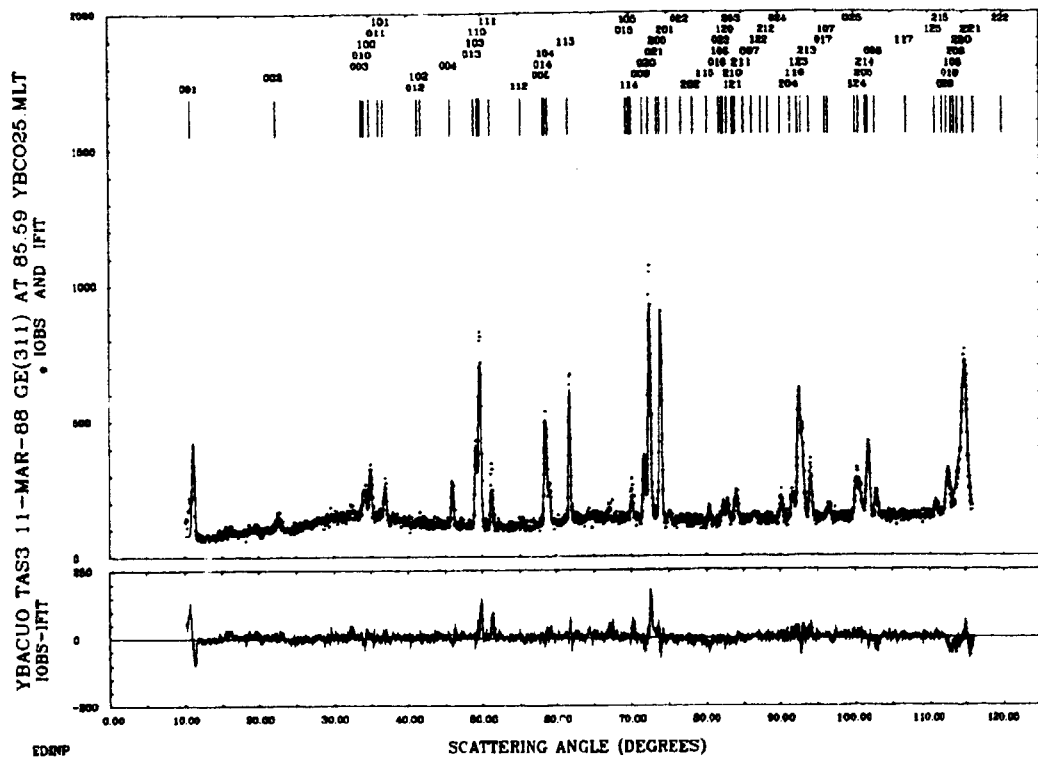


Fig. 3. Powder diffraction pattern from  $YBa_2Cu_3O_{7-x}$  obtained with a  $Ge(311)$  monochromator at  $2\theta_M = 85.6^\circ$  ( $\lambda = 2.32 \text{ \AA}$ ). The counting time for the full pattern was about one hour. Top: Observed (.....) and profile refined (—) patterns. Bottom: Difference between the observed and calculated patterns.

scattering plane, neither of the incident beam nor of the Bragg scattered beam. Accordingly we use (i) a rather high monochromator crystal subtending the full height of the reactor beam and bent to partially focus the beam in the vertical plane onto the sample, and (ii) a rather high detector to subtend as much as practically possible of the Debye-Scherrer cone. Second, the transmission of the collimators defining the direction of the incident and scattered beams should be high.

The necessary angular resolution to separate Bragg peaks at wave vector transfers around  $9 \text{ \AA}^{-1}$  is around  $10'$  or 3 milliradians using a wave vector around  $4 \text{ \AA}^{-1}$ . This could be obtained by 1 mm wide slits 30 cm apart, but the sample width is usually much wider than 1 mm, so in order to take advantage of the available sample size (width) we use a multi-slit collimator, a so-called Soller collimator. It consists of a set of channels separated by thin, but strongly neutron absorbing walls. The wall thickness

relative to the channel width determines the loss in transmission. Third, by using a bank of  $N$  detectors each having Soller collimator pointing towards the sample one reduces the data acquisition time by  $1/N$  compared to a single detector system. In the present case we use a detector bank of twenty detectors spanning an angular range of about  $100^\circ$ . The full diffraction pattern shown in Fig. 3 is then obtained by 100 angular settings of the detector bank yielding 2000 data points.

Having now described the basic features of the powder diffractometer we shall in the following sections discuss the individual components in more detail. A summary of the components of the diffractometer are given in appendix A1.

## 2. Monochromator

### 2.1. Lattice Spacing

As discussed in the previous section one should use a large Bragg angle at the monochromator. With the present monochromator shielding and space in the DR3 reactor the maximal value of  $2\theta_M$  is  $90^\circ$ . The thermal Maxwellian spectrum peaks around 40 meV and the corresponding value of  $k$  is around  $4 \text{ \AA}^{-1}$ . From Eq. (1) with  $\theta_M = 45^\circ$  we then find  $\epsilon_M$  should be approximately  $6 \text{ \AA}^{-1}$  which corresponds to a lattice spacing of around  $1 \text{ \AA}$ .

### 2.2. Higher Order Contamination

The monochromatic beam should not be contaminated by higher order reflections relative to the dynamic range of approximately 100:1. The higher harmonic wave vectors  $2k$ ,  $3k$  etc. correspond to energies of 4,9 etc. times the primary energy. The reactor spectrum implies that only second harmonic contamination may present a problem. It may be overcome by using a monochromator reflection where the second order reflection is forbidden. The concept of forbidden reflections may be understood from Eqs. (3) and (4). Assume that the monochromator only have one kind of atoms, all with the same thermal vibration amplitude. The structure factor in Eq. (3) is then simply a summation over phase factors. The reader may easily verify that in an f.c.c. unit cell only reflections with all indices either even or odd are non vanishing.

The diamond structure can be considered as two interpenetrating f.c.c. lattices displaced  $1/4$  of a cube diagonal. In addition to the f.c.c. selection rule the diamond lattice therefore implies that  $(1 + \exp(i\pi/2(h+k+\ell)))$  must be non vanishing. In particular, if  $(h,k,\ell)$  are all odd, the sum is odd. Therefore, the reflection is allowed, but the second order  $(2h,2k,2\ell)$  has an even sum so the second order reflection is forbidden. Semiconductors such as Si and Ge have the diamond structure and they can be

grown as large crystals. We have chosen to use a Ge monochromator crystal which can be oriented to reflect from the  $(h, \ell, \ell)$  planes. For  $\ell = 1$  and odd  $h = 1, 3, 5, 7$  etc. one obtains reflections where second order is forbidden. The  $\nu_{511}$  reciprocal lattice vector has a length of  $5.7709 \text{ \AA}^{-1}$  which is a convenient magnitude.

### 2.3. Mosaicity

Semiconductor crystals have however one drawback as monochromator crystals: they are too perfect. The monochromator crystal should have a mosaic spread at least of the same order of magnitude as the collimation between monochromator and sample, i.e.  $10'$ , in order to utilize as broad a wavelength band as possible of the reactor spectrum without significantly deteriorating the powder spectrum resolution. It is possible to obtain such a mosaic spread artificially in a Ge crystal by applying a uniaxial pressure at elevated temperatures. Our monochromator Ge crystal was prepared in such a way by the Crystal Laboratory at Institute Laue Langevin, Grenoble, France and obtained a mosaicity of about  $10'$  FWHM (Full Width at Half Maximum).

### 2.4. Sagittal Focussing

In addition to having an appropriate lattice spacing, mosaicity and forbidden second order, the monochromator crystal should also focus spatially in the vertical plane so that the 10 cm high reactor

beam is focussed to a height of a few centimeters at the sample position, i.e. the top part of the crystal should reflect the reactor beam downwards and the bottom part should reflect it upwards. A monolithic Ge crystal cannot be bent to provide this so-called sagittal focussing, it is too brittle. Consequently we cut our pressed Ge monolithic crystal into smaller pieces:  $12 \times 12$  mm  $(3,1,1)$  faces that are 8 mm thick. Out of these pieces we selected 21 crystals with similar mosaicity and mounted them in the monochromator holder in a  $3 \times 7$  array so that each of them could be tuned to the appropriate orientation in a test beam. Once correctly oriented they were fixed by embedding in epoxy so the final monochromator assembly has a fixed radius of curvature for the sagittal focussing. However, the final radius of curvature is not very critical because the neutron source in the reactor is quite extended and hence the focussing effect is considerably blurred in practice. Therefore all the  $(h,1,1)$  reflections with  $h=1,3,5$  and 7 have approximately sagittal focussing.

## 3. Collimators

The direction of the incident and scattered beam is determined by multi-slit collimators, so-called Soller collimators. The angular divergence is  $10'$  obtained by a slit width of 1.0 mm and a length of 320 mm. The height of each slit

is 100 mm. The slit walls should be thin in order to obtain a high transmission of the Soller collimator, but at the same time highly neutron absorbing so that cross-talk between slits can be neglected. We manufactured walls of a 0.012 mm thin plastic foil coated on both sides with approximately 0.03 mm paint in which the strongly neutron absorbing material  $Gd_2O_3$  was dissolved in an amount of 250 g/l. The transmission through such a wall at a glancing angle of  $2 \times 10'$  is around  $10^{-8}$  at  $1 \text{ \AA}$ , so cross-talk between channels is eliminated. The channel width is provided by spacers at the top and bottom of the channel. A special tool was developed to mount the stack of coated plastic foils and spacers in a stainless steel frame so that all foils are straight and accurately parallel to the outer edge of the steel frame.

As indicated in Fig.1 each of the twenty detectors has a collimator in front. However, we have a separate mounting of the detectors and collimators into a collimator bank and a detector bank for the following reasons. The detectors need a substantial amount of shielding around to reduce the stray neutron background to an acceptable level. As shielding material we use an epoxy with a neutron absorbing boron compound so that fast neutrons are being moderated and then absorbed. Test of this detector shielding material indicates that a shielding thickness of about 20 cm is required on all sides around the detector. This means

that the shielding around the detector bank is a bulky entity weighing around 400 kg and it would therefore not be trivial to move the detector bank around with a precision of a fraction of the collimation width, say by a precision of  $1'$ . However, the detector response is quite flat across the detector window, so if just the collimator bank is moved precisely one can relax on the precision of the movement of the detector bank. There is a further advantage of separate collimator and detector banks. In a fixed beam, e.g. the incident beam properly attenuated or on a powder diffracted beam one can *scan* the entire collimator bank in front of a *fixed* detector and thereby experimentally find possible errors in the equidistant mounting of the collimators. The collimators were mounted on a counter weight balanced turntable with a nominal angular separation of  $5.289^\circ$ . The collimator bank scan over an angular range of  $20 \times 5.289^\circ = 105.8^\circ$  with fixed detector gave a maximal error of  $0.025^\circ$  and a standard deviation of  $0.015^\circ$ . These numbers are so small compared to the collimation width of  $10'$  or  $0.167^\circ$  that the collimators for all practical purposes can be considered as rigidly equidistant. In setting up a powder pattern scan the angle between neighboring collimators is divided into a number of steps, so in the last point of the scan collimator  $n$  is precisely one step from the starting angle of collimator  $n + 1$ .

## 4. Detectors and Electronics

The twenty detectors are He<sup>3</sup> filled gas proportional counters manufactured by LND, Inc., New York, USA. The He<sup>3</sup> pressure of 5 atm. together with a thickness of 2 cm gives an efficiency of 63% at a wavelength of 1.3 Å. The sensitive area is 2 cm wide by 10 cm high. The detectors all have the same gas filling and they are in fact quite similar in efficiency. Right on top of the detector bank and within the shielding is mounted a pre-amplifier bank, the advantage of the proximity being an improved signal to noise ratio due to the minimal capacitance. Output signals from the twenty preamplifiers are led to a bank of main amplifiers and single channel analysers outside the shielding. Each main amplifier can be tuned by a potentiometer to provide a pulse height of 4 V and a pulse width of approximately 3 μs. All Single Channel Analysers are set to provide a standard TTL pulse for an input pulse between 0.75 V and 4.5 V. The SCA output on 20 lines are then fed into a decoder providing an interface to the computer. The detector electronics is described in some detail in appendix A2.

## 5. Powder Spectrum Resolution

The width of a powder line, c.f. Fig. 3, is partly determined by the collimators

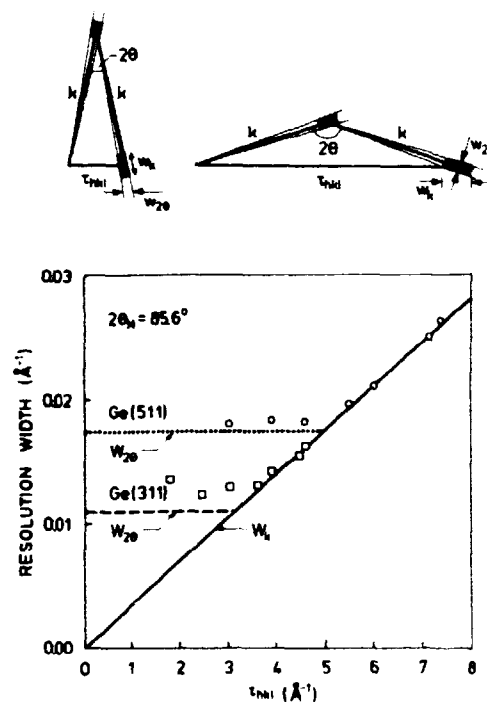


Fig. 4. Top: The resolution width (FWHM) in a powder spectrum is at small angles mainly determined by collimation ( $W_{20}$ ), but at large angles mainly by monochromaticity ( $W_k$ ). Bottom: Comparison of measured resolution widths from a standard Al<sub>2</sub>O<sub>3</sub> powder with Eqs. (6) and (7).

determining the direction of the incident and scattered ray, and partly by the wavelength spread of the monochromatic beam. In Fig. 4a is depicted two extreme cases: At very small angles the width,  $W$ , is determined by collimation only ( $W = W_{20}$ ), whereas in the opposite extreme case of large scattering angles the width is determined solely by the relative wave vector spread  $\delta k/k$  ( $W = W_k$ ). If the entrance and exit collimators have identical widths  $\sigma$ , then

$$W_{2\theta} = k\sqrt{2\sigma} \quad (6)$$

whereas the width  $W_k$  follows by differentiating the relation  $\nu_{hkl} = 2k\sin(\theta_{hkl})$

$$W_k = \nu_{hkl}(\delta k/k) \quad (7)$$

The relative wave vector or wavelength spread  $\delta k/k$  is

$$\delta k/k = \delta\theta_M / \tan(\theta_M) \quad (8)$$

In Fig. 4b  $W_{2\theta}$  and  $W_k$  are compared to experimental widths from an  $Al_2O_3$  standard powder sample using either the (311) or the (511) reflections of the Ge monochromator crystal set at  $2\theta_M = 85.6^\circ$ . In plotting  $W_k$  we have used  $\delta k/k = 0.35\%$  corresponding to  $\delta\theta_M = 11'$ ,

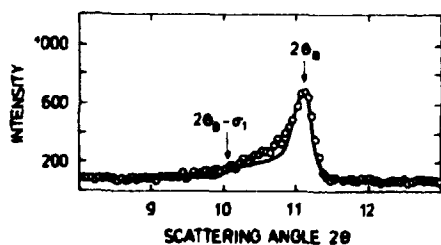


Fig. 5. At low angles the combination of straight Soller collimators and curved Debye-Scherrer cones implies a line shape with a tail on the low angle side. The full curve is calculated as described in appendix A3.

which is quite a reasonable value given the  $10'$  collimation between monochromator and sample and the effective mosaicity of the monochromator crystal. Note that the slope of  $W_k$  versus  $\nu_{hkl}$  is inversely proportional to  $\tan(\theta_M)$  showing the advantage of using a high take-off angle from the monochromator to obtain good resolution at large wave vector transfers.

The discussion above of resolution at very large and very small angles assumed that the *vertical* resolution can be neglected in the sense that the part of the Debye-Scherrer cone contributing to the scattering can be approximated by a vertical line. However, at very small and at large scattering angles, the Debye-Scherrer cone is indeed very concave, and that may affect the observed line shape. At small angles this will lead to a tail on the low angle side of a powder peak and at large angles to a tail on the high angle side. An example is given in Fig. 5 showing a powder peak at  $2\theta_S = 11^\circ$ . The full detector height was 10 cm which together with a sample to detector distance of 60 cm leads to an azimuthal angular range on the Debye-Scherrer cone of as much as  $-25^\circ$  to  $+25^\circ$ . A quantitative evaluation of the line shape is given in appendix A3 and shown as the full curve in Fig. 5.

## 6. Software

The powder diffractometer is controlled by a PDP11-23 computer under the multi-user TSX-11 operating system, and is equipped with a hard disc, two floppy discs, a standard video display (VDU) and a graphics screen. The control programme is an extended version of the TASCOM programme used in general for Risø neutron- and x-ray spectrometers. The extension handles the twenty separate detectors used for the powder diffractometer. However, the programme can still operate on any single one of these detectors, which is a useful option for line-up purposes and special investigations of selected powder peaks. It is therefore useful to divide this section into single detector mode and multi-detector mode.

### 6.1. Single Detector Mode

Very briefly, the main purpose in this mode is for a selected detector in the detector bank to carry out the following sequence of instructions :

- (i) to set the detector at a given scattering angle,
  - (ii) to measure for a certain time or for a preset accumulated number of counts in the monitor channel,
  - (iii) to print the result in a user determined format on the screen and printer
- iv) to move to the next point in a user defined angular scan and repeat (i)-(iii),
  - (v) by completion of the scan to provide a x-y plot in user-defined assignments of (x,y), to find peak position and width if the data can be interpreted in terms of a peak, to store the data of the scan in a datafile on disc and to up-date the file number by one.

We will assume that the reader is familiar with the general operation of TASCOM or refer to the TASCOM manual. Here we shall only recall the special features of single detector mode on the powder spectrometer by explaining the function of a few variables.

**CHAN** CHANNEL number or detector number in the range 1-20, c.f. Fig.1. The accumulated intensity in this detector is as usual denoted I.

**TTC** Two Theta of Channel CHAN in degrees.

**PLTY** provides labelling of axes etc. in the plot. Must be set to "SNGD" in SiNGle Detector Mode.

**Q** The wave vector transfer seen by detector number CHAN.

**CQ** Is +1 for scattering to the left, -1 for scattering to the right, when following the neutrons from the source.

**CO56** Coupled movement of detector bank (motor 5, 100 steps/degree) and collimator bank (motor 6, 2000 steps/degree). Its value is 1 for coupled movement (with approximately the same speed of the two banks) and 0 for independent movement of motor 5 and 6.

## 6.2. Multi Detector Mode

In this mode the computer has to handle the intensities from all twenty detectors. The input comes from the twenty-detector decoder described in section 4. The amount of data is large and is therefore stored on disc in compact, so-called "unformatted" files. Such a data-file of type <filename.MLT> contains a user defined file text and date, the angular offset of each of the twenty detectors (in practice the offsets are all 0, c.f. section 3) and the relative efficiency of each detector (in practice all unity). Then follows the first angular setting and the corresponding twenty intensities, the second angular setting and the corresponding twenty intensities and so on. A program outside TASCOM called MANMLT translates an MLT file to an ASCII file. Typical file sizes for 100 angular settings are 17 blocks for the MLT file and 110 blocks for the ASCII file. In addition to provide ASCII format the MANMLT program also sorts the data in sequence of increasing angles, which is a useful feature when an ASCII file is the database for plotting routines,

structure refinement, etc. On-line monitoring of the powder spectrum as it is being accumulated, is provided on the graphics screen. There are a number of options concerning scaling of the plots as explained below.

By completion of the scan, the screen picture is dumped on the printer and with TASCOM commands it is also possible at this stage to plot for example one or more sections of the full spectrum without translating the file into ASCII format. Special commands and variables in the Multi Detector Mode include:

- PLTY** must be set to "MLTD" in the Multi Detector mode.
- LOOK** = 1 if on-line graphics is to appear on the screen during data accumulation. The command PLOT (see below) is disabled.  
= 0 to disable on-line graphics. The command PLOT (see below) is enabled.
- PLOT** plots the accumulated data (in MLT format), according to the scaling criteria set by LIMX and LIMY, provided LOOK = 0.
- LIMX** = 1, user assigned values of XMIN and XMAX  
= 2, automatic value of XMAX, XMIN = 0.  
= 0, automatic values of XMIN and XMAX..



LIMY = 1, user assigned values to YMIN and YMAX.  
 = 2, automatic value of YMAX. YMIN = 0.  
 = 0, automatic value of YMIN and YMAX.

VT24 = 1 for a graphics scan (ex. VT240 or VT340).  
 = 0 for any other terminal (disabling graphics plots).

mechanical alterations to the spectrometer, or a new monochromator reflection has been chosen, or there are other reasons to disbelieve the present zero angles, a new determination of these should be carried out. This process as well as ensuring that the monochromator is reflecting a monochromatic beam optimally onto the sample, is called lining up the spectrometer.

## 7. Lining-Up the Multi-Detector Diffractometer

Any angle determination is a relative measurement. The reference angle or zero angle of each angle measurement must therefore be known to sufficient accuracy. Any time there have been

Each element of the spectrometer must be lined up without requiring knowledge of the yet unknown parameters of the remaining elements. This makes the natural direction of the line-up procedure follow the neutron beam through the spectrometer. Each step in this process are described in the following.

Ge reflection	$\tau_M$	fast rotation negative time/s	count rate/kcps M1 = 8560
(133)	4.84104	0	7.5
(111)	1.92363	23	20.0
(533)	7.28276	37	8.6
(422)	5.44086	43	20.0
(733)	8.95402	47	4.5
(311)	3.68348	53	17.0
(822)	9.42384	59	5.0
(511)	5.77090	63	16.0
(711)	7.93134	67	7.0
(400)	4.44244	78	20.0

Table 1. Characteristics of reflections from the Ge monochromator. Column 3 is the time taken by the manually operated rotation device to rotate between the various reflections. This time may be used in connection with column 4 to find the desired monochromator reflection. The count rates in column 4 are from a fission monitor at TAS3.

To ensure a rapid and well defined line-up of the spectrometer the computer which controls the spectrometer may guide the user through this process. A reproduction of the computer output during such a line-up procedure is given in appendix A4.

### 7.1. Monochromator

The monochromator must be rotated so the desired reciprocal lattice vector halves the angle that the monochromator scattering angle is set to. It must also be assured that the reciprocal lattice vector lies in the horizontal scattering plane of the spectrometer. The standard Ge monochromator is as noted earlier oriented in the  $(h, \ell, \ell)$  plane. As a help to identifying the desired reflection Fig. 6 shows the reciprocal lattice vectors with an appreciable associated reflectivity in this plane. The monochromator is

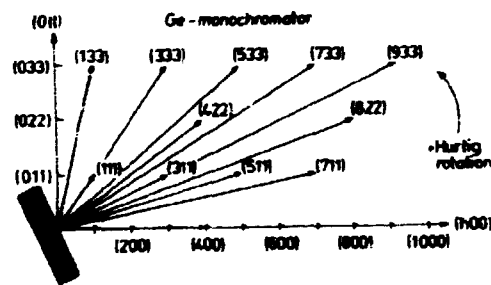


Fig. 6. Reflections with appreciable intensity from the Ge monochromator mounted in the  $(h, \ell, \ell)$  plane. The arrow indicates the sequence in which the reflections appear when rotating in the positive direction on the monochromator rotation device.

rotated by a manually operated motor drive unit with no absolute encoder. The time taken to rotate between two reflections can, however, be used to identify them (see Table 1). Once the desired reflection has been identified the countrate on a monitor placed immediately at the exit from the monochromator drum is optimized by rotating and tilting the monochromator with the manually operated motor drive.

### 7.2. Monochromator-Sample Collimator

The next step is to align the monochromator-sample collimator (CO in Fig. 1) parallel to the direction of the beam from the monochromator. For this purpose the monitor is placed immediately after the collimator, which is mounted on a rotation device which is then rotated until maximum intensity is transmitted through the collimator CO. At this step a monochromatic collimated incident neutron beam has been prepared.

### 7.3. Sample Table Alignment

The centre of the sample table must now be centred in the incident beam. This is done by moving a strong incoherent scatterer (a perspex rod) placed on the sample table through the incident beam while monitoring the total countrate of all twenty detectors. The position at which the intensity is maximal corresponds to the sample being centred in the incident beam. After completing

this step we have centred the sample table in the collimated monochromatic incident beam.

#### 7.4. Sample Scattering Angle

The zero angle of the sample scattering angle is now determined by scanning one detector through the attenuated incident beam. This zero angle may also be measured by scanning through the powder peaks corresponding to scattering to right and left from a powder sample. The zero angle is then the bisecting direction in between these two directions.

#### 7.5. Detector-Bank Collimator Alignment

The alignment of the detector-bank with respect to the collimators (C1, C2,... in Fig. 1) is established by scanning a detector through the incident beam after this has passed through the corresponding collimator. The detectors are placed behind their respective collimators when this intensity is optimized.

#### 7.6. Monochromator Scattering Angle

Finally the scattering angle at the monochromator, and thereby the neutron wave vector  $k$  (see Eq. 1), is determined by measuring the scattering angle of a powder peak of an aluminum

oxide standard sample. From Bragg's law the following equation holds

$$\frac{\tau_S}{\tau_M} = \frac{\sin\theta_S}{\sin\theta_M}$$

where  $\tau_S$ ,  $\theta_S$  are the reciprocal lattice vector and half scattering angle at the sample, and  $\tau_M$ ,  $\theta_M$  are the corresponding values for the monochromator. So by measuring  $\theta_S$  for the known values of  $\tau_S$  and  $\tau_M$  we find the scattering angle at the monochromator

$$2\theta_M = 2\text{Arcsin}\left(\frac{\tau_M}{\tau_S} \sin\theta_S\right)$$

## 8. Example of a Structure Study

Shortly after the discovery of the ceramic superconductors at the end of 1986 it was realized that the occurrence of high temperature superconductivity is closely related to the properties of the copper-oxygen bonds. Structural studies are therefore very important in the search for the basic principles of high- $T_c$  superconductivity as well as a number of materials properties related to applications.

Since the ceramic high- $T_c$  superconductors are available so far mainly as powder samples, and important structural features are related to minor crystalline distortions of almost tetrago

nal structures, there is a need for a high resolution spectrometer. Many aspects related to synthesis and studies of kinetics in the structural transformations call for short measuring times. The multi-detector high-resolution powder neutron diffractometer was designed and constructed to meet these requirements. As an example some studies of the structural properties connected to the oxygen stoichiometry in  $\text{YBa}_2\text{Cu}_3\text{O}_{7-x}$ , will be mentioned. A neutron wavelength of  $\lambda = 2.32 \text{ \AA}$  obtained with a Ge(311) monochromator at  $\theta_M = 85.6^\circ$  was used for the measurements.

### 8.1. Phase Equilibrium and Kinetics of the Oxygen Uptake of $\text{YBa}_2\text{Cu}_3\text{O}_{7-x}$

For  $x < 0.5$ ,  $\text{YBa}_2\text{Cu}_3\text{O}_{7-x}$  has an orthorhombic structure as shown in Fig. 2. The temperature variation of the lattice parameters are shown in Fig. 7. At room temperature almost full oxygen occupancy in the crystalline lattice is found on the sites O(1), O(2), O(3), and O(4) in Fig. 2, whereas site O(5) is essentially empty. On heating, deviations from stoichiometry occur and result in a partial occupancy on the O(1)-site. Simultaneously the O(5)-site becomes increasingly populated. At temperatures above  $660^\circ\text{C}$ , sites O(1) and O(5) are equally populated and the crystal structure transform from orthorhombic to tetragonal. If non-stoichiometric  $\text{YBa}_2\text{Cu}_3\text{O}_{7-x}$  is quenched from high temperatures or cooled in vacuum, the

non-stoichiometry remain, and the superconducting properties are significantly deteriorated. For  $x$  approaching 1 superconductivity disappears and antiferromagnetic order is observed. It is therefore important to study the conditions for phase equilibrium and the kinetics of oxygen uptake in this system.

Three sequences in studies related to these properties of  $\text{YBa}_2\text{Cu}_3\text{O}_{7-x}$  should be mentioned. First, when heated in 100% oxygen the orthorhombic lattice expands as shown in Fig. 7. At temperatures above  $600^\circ\text{C}$  the a- and b-axes starts to approach each other and a phase transition to the tetragonal structure is observed at  $670^\circ\text{C}$ . As mentioned the

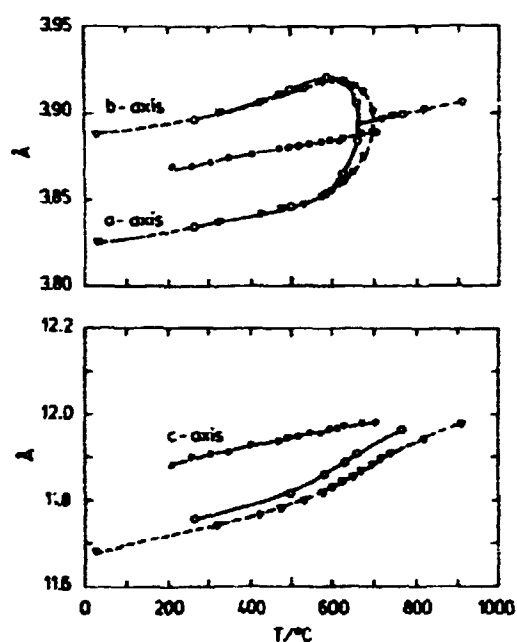


Fig. 7. Temperature variation of the lattice parameters in  $\text{YBa}_2\text{Cu}_3\text{O}_{7-x}$ . Open symbols refer to heating in 100%  $\text{O}_2$ ;  $\nabla$  Jorgensen et al.,  $\circ$  our data,  $\bullet$  our results, cooling under vacuum from above  $700^\circ\text{C}$ .

phase transition is driven by the depletion of oxygen from site 0(1) and disordering by occupancy on site 0(5) (Fig. 2). These properties may be determined from structural refinements on the full powder spectrum shown in Fig. 3. However, it is worth mentioning that the depletion of oxygen from the basal plane sites 0(1) and 0(5) may be studied qualitatively from the intensity of the (001)-peak found at  $2\theta = 11.3^\circ$  in the powder diffraction pattern. In a 100% oxygen atmosphere Jorgensen et al. (Phys. Rev. B36, 3608 (1987)) have determined an equilibrium oxygen concentration corresponding to  $x = 0.58$  at  $818^\circ\text{C}$ . Structural refinements on our data have not yet been completed. Although, there are some differences in the lattice constants obtained in our study and that of Jorgensen et al. (see Fig. 7), we expect a qualitatively similar behaviour.

The lattice expands on heating despite the loss of oxygen. Actually, the loss of oxygen contributes as a driving mechanism in the expansion of the lattice. This is also seen from the experimental results shown in Fig. 7, where the sample has been evacuated in the tetragonal phase above  $700^\circ\text{C}$  with a significant expansion of the c-axis as a result. A semi-quantitative evaluation of the stoichiometry, based on the (002)-peak intensity, indicates an equilibrium stoichiometry in vacuum at these temperatures corresponding to  $\text{YBa}_2\text{Cu}_3\text{O}_6$ . Subsequent cooling under vacuum maintain the

tetragonal phase and the oxygen deficiency. At room temperature the oxygen deficient tetragonal phase has proven to be stable in air for more than a week.

A third experiment has been performed in order to study the kinetics of the oxygen uptake towards equilibrium. The sample being cooled under vacuum from  $700^\circ\text{C}$  to room temperature, and thereby maintained in the oxygen deficit tetragonal phase, was heated semi-dynamical with an increase of  $25^\circ\text{C}$  every two hours, and the transformation towards the orthorhombic equilibrium phase was

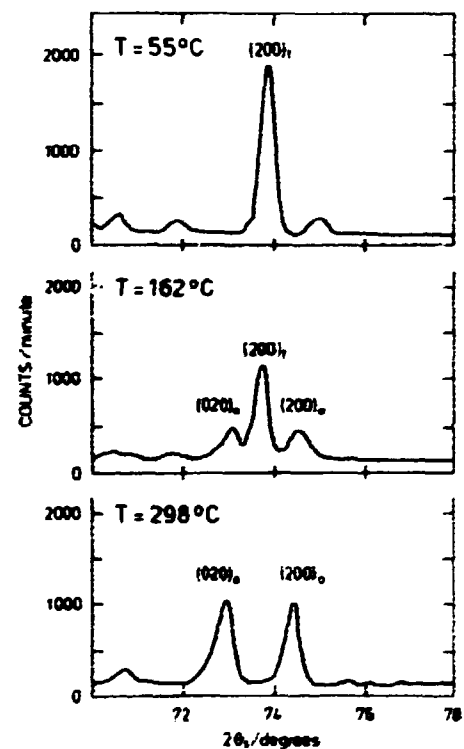


Fig. 8. Tetragonal  $(200)_t$  - and orthorhombic  $(020)_o$ - and  $(200)_o$ -Bragg-peaks used to study the transformation between tetragonal and orthorhombic phase.

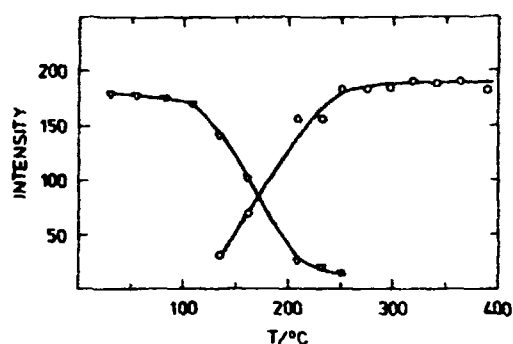


Fig. 9. Temperature variation of the Bragg-peak intensities of:  $\nabla$  - the tetragonal  $(200)_t$ -peak,  $\circ$  - the sum of orthorhombic  $(020)_o$ - and  $(200)_o$ -peaks.

studied. From a study of the tetragonal  $(200)$ -peak, which splits into close-lying  $(200)$ - and  $(020)$ -peaks in the orthorhombic phase shown in Fig. 8, it is observed that only these two phases are present during the transformation. This indicates that the transformation occurs via a diffusion process through the orthorhombic phase developing from the surface of the grains of the ceramic sample. The temperature variation in the tetragonal  $(200)$ -peak intensity and the sum of orthorhombic  $(200)$ - and  $(020)$ -peak intensities are shown in Fig. 9. The results show that the annealing process leading to oxygen equilibrium in  $\text{YBa}_2\text{Cu}_3\text{O}_{7-x}$  may be performed at temperatures as low as  $200^\circ\text{C}$ , which is significantly lower than usually recom-

mended e.g. during synthesis. An isothermal annealing process performed at  $165^\circ\text{C}$  showed that 75% of the sample was transformed from the tetragonal to the orthorhombic phase within fifty hours. Further studies of these properties are in progress.

### Acknowledgements

The powder diffractometer was constructed by J. Linderholm and the crystal orientation device by K. Theodor. The assembling and installation of the mechanical parts were done by L. G. Jensen and T. Kjær. The production of mechanical parts at the Risø Central Workshop and the electronics at Electronics Department within a very short time are much appreciated. The Ge monochromator crystal was pressed at the Institute Laue Langevin, Grenoble, France by Drs. A. Freund and B. Hamelin at ILL and Mr. T. Lorentzen from Risø. The data analysis of the kinetics of  $\text{YBa}_2\text{Cu}_3\text{O}_{7-x}$  was done by Mr. H. Friis Poulsen. We have benefitted from enlightening discussions with Dr. M. Lehmann from Institute Laue Langevin.



## Appendix A.1. Summary Sheet for the Risø Powder Diffractometer

### A.1.1. Monochromator

Ge: Diamond structure,  $a = 5.6574 \text{ \AA}$

Mounting:  $3 \times 7$  Pressed Ge crystals of dimensions:  $12 \times 12 \times 8 \text{ mm}^3$  with (311) perpendicular to the surface mounted on a Gd shielded vertically curved Al holder.

Relative structure factors (F): 1 for  $h+k+l = 4n$  ( $h,k,l$ ) all even  
0.7071 for ( $h,k,l$ ) all odd  
0 all other combinations of ( $h,k,l$ )

Mosaicity:  $10'$  (FWHM)

For  $90^\circ$  take off angle at the monochromator:

mono-chromator reflection	wave-length $\text{\AA}$	wave vector $\text{\AA}^{-1}$	energy meV	Q-range $\text{\AA}^{-1}$ for $5^\circ$ - $110^\circ$ in $2\theta$
(111)	4.6192	1.3602	3.83	0.12-2.23
(311)	2.4123	2.6046	14.06	0.23-4.27
(511)	1.5397	4.0807	34.50	0.36-6.69
(711)	1.1203	5.6083	65.17	0.40-9.19
(911)	0.8782	7.1546	106.07	0.62-11.72

### A.1.2. Collimators

The collimator-bank before detector bank consists of twenty Soller collimators with collimation  $10'$  and separation  $5.289^\circ$ .



Collimator sheets: Gd coated mylar-foil

Transmission through a single foil:

angle	transm. (1 Å)	transm. (2 Å)
90°	0.92	0.85
10'	$7 \cdot 10^{-13}$	$5 \cdot 10^{-25}$
20'	$9 \cdot 10^{-7}$	$7 \cdot 10^{-13}$

Collimation: Reactor - Monochromator 15', 30' or 60'  
Monochromator - Sample 10'  
Sample - Dectector 10'

### A.1.3. Detector-bank

20 single  $^3\text{He}$  detectors: LND, Inc. type 2624

$^3\text{He}$  pressure 5 atm

Effective volume  $20 \times 20 \times 100 \text{ mm}^3$

High Voltage 1300 V

Gas amplification  $\approx 15$

Separation between Detectors 5.289°

## **Appendix A.2. Electronic Set-Up**

### **A2.1. TAS3 - Set-Up**

**Beam:** Thermal

**Special features:**

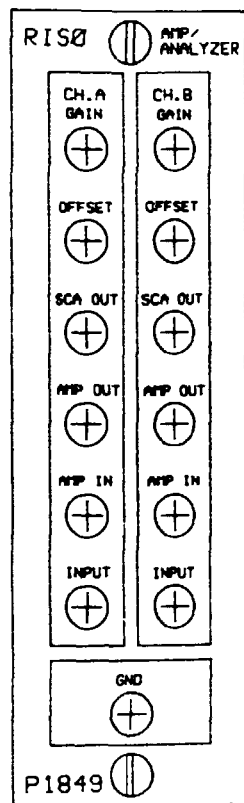
	motor	No. of steps/degree
Detector bank	M5	100
Collimator bank	M6	2000

**NB:** The following cables should be checked:

- 1) In the CAMAC CRATE there should always be a cable from the upper INH ALL in the HYTEC module to the back of the MATRIX encoder in the NIM bin.
- 2) On the top of the MOTOR DRIVE cupboard cable 240 should be connected to the left most unit and cables 333 and 142 to the adjacent motor unit.

### **A.2.2. Detector electronics**

- 1 Single High-Voltage supply.
- 20 Pre-amplifiers mounted directly on top of the Detectors.
- 10 Double amplifier/SCA (Single Channel Analyser) units. DC-offset and gain can be adjusted individually for all 20 amplifiers.
- 1 Power module with potentiometers for setting of a common lower and upper limit for all twenty SCA.



**Adjustment of amplifier/SCA P1849:**

*Fig. 10. Double Amp/SCA module*

*Adjust gain so that the maximum peak-height for the signals is 4 V.*

*Adjust offset so that background is 0 V.*

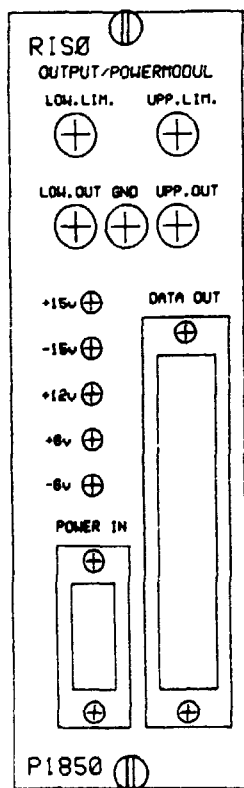
*Connect oscilloscope to terminals GND (ground) and AMP OUT.*

*Oscilloscope settings:  
Vertical 1V/division DC*

*Timebase 1  $\mu$ s/division*

*Trig Coupl DC*

*Trig mode TRIG*



**Adjustment of common discriminator levels for the SCA's P1850:**

*Fig. 11. Power module*

*Adjust the lower limit so that it exceeds the electronic noise level.*

*Typical setting 0.7-1.0 V.*

*Adjust the upper limit so that it exceeds the 'neutron' pulse height.*

*Typical setting 4.5-5.0 V.*

*Connect oscilloscope to terminals GND (ground) and LOW.OUT or UPP.OUT, respectively.*

*Oscilloscope settings:*

*Vertical 1V/division DC*

*Timebase Irrelevant*

*Trig Coupl DC*

*Trig mode AUTO*

## Appendix A.3. Powder Line-Broadening due to Vertical Divergence

### A.3.1. Problem

A crystalline powder scatters a horizontal monochromatic beam into a Debye-Scherrer cone of opening angle  $2\theta$  (see Fig. 12). For the special case of  $2\theta = 90^\circ$  the cone is degenerated into a vertical flat disc. In that special case the *horizontal* component of the scattered ray is independent of the azimuthal angle  $t$  around the Debye-Scherrer cone. But for  $2\theta < 90^\circ$  this horizontal component is *less* than  $2\theta$ , whereas for  $2\theta > 90^\circ$  the horizontal component is *larger* than  $2\theta$ . In a powder diffractometer with vertical Soller slits before the detector, the powder line will be broadened to the low angle side for  $2\theta < 90^\circ$  and similarly to the high angle side for  $2\theta > 90^\circ$ . It is the purpose of this appendix to calculate the corresponding powder line-shape.

### A.3.2. Quantitative Evaluation

The incident, horizontal wave vector  $\mathbf{k}_i = \mathbf{OR}$  is Bragg scattered through angle  $2\theta$  in the horizontal plane to wave vector  $\mathbf{k}_f = \mathbf{OQ}$ , the wave vector transfer  $\mathbf{t}$  being a reciprocal lattice vector of a particular grain in the powder (see Fig. 12). Since the problem is entirely geometric we can choose our units of reciprocal space so that  $|\mathbf{k}_i| = |\mathbf{k}_f| = 1$ . In general the scattered wave vector  $\mathbf{k}_f$  is *not* horizontal but is somewhere on the Debye-Scherrer cone, say along  $\mathbf{OP}$  with azimuthal angle  $t$ . The projection of  $\mathbf{OP}$  on the horizontal plane is  $\mathbf{OP}'$ . The Cartesian coordinates of  $\mathbf{OP}$ ,  $\mathbf{OP}'$  and  $\mathbf{OQ}$  are

$$\begin{aligned}\mathbf{OP} &= (\sin 2\theta \cos t, \cos 2\theta, \sin 2\theta \sin t) \\ \mathbf{OQ} &= (\sin 2\theta, \cos 2\theta, 0) \\ \mathbf{OP}' &= (\sin 2\theta \cos t, \cos 2\theta, 0)\end{aligned}$$

The vertical angle  $v$  of the scattered ray  $\mathbf{OP}$  is given by

$$\sin v = \sin 2\theta \sin t \quad (\text{A1})$$

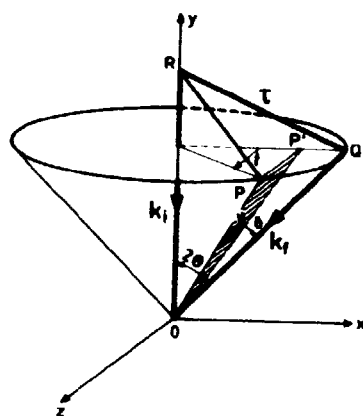


Fig. 12. Scattering geometry used to calculate the diffraction line-profile from a Debye-Scherrer cone for a high detector.

and the length of  $OP'$  is simply  $\cos \nu$ .

The angular *difference* in the horizontal plane between  $OP'$  and  $OQ$  is denoted  $\delta$ , and we want to determine  $\delta$  for given values of  $\nu$  and  $2\theta$ . This is easily done by evaluating the scalar product of  $OP'$  and  $OQ$ :

$$OP' \cdot OQ = \cos \nu \cdot 1 \cdot \cos \delta$$

or

$$\cos \nu \cos \delta = |1 - (1 - \cos t) \sin^2 2\theta| \quad (A2)$$

Let us, for brevity denote  $\sin 2\theta$  by  $\alpha$ :

$$\alpha = \sin 2\theta \quad (A3)$$

The angles  $\nu$  and  $t$  are small, and by series expansion one obtains from Eq. (A1) the approximate relation

$$\nu(t) \approx \alpha t \{1 - t^2/6 (1 - \alpha^2)\} \quad (A1a)$$

Equation (A2) is evaluated in a similar manner resulting in

$$\delta(t) \approx (t^2/2) \alpha (1 - \alpha^2)^{-1/2} \quad (A2a)$$

when utilizing the result of Eq. (A1a).

The detector can only accept vertical angles less than a certain limit  $v_1$  set by the detector height  $Z$  and the distance  $R$  to the sample:

$$|v| \leq v_1 \quad \text{with } \tan v_1 = Z/(2R) \quad (\text{A4a})$$

The corresponding maximal azimuthal angle  $t_1$  is derived from Eq. (A1)

$$\sin t_1 = \alpha^{-1} \cdot \sin v_1 \quad (\text{A4b})$$

and the corresponding maximal angle  $\delta, \delta_1$ , from Eqs. (A1) and (A2) is given by

$$\cos v_1 \cos \delta_1 = |1 - (1 - \cos t_1) \alpha^2| \quad (\text{A4c})$$

The scattered intensity is evenly distributed around the Debye-Scherrer cone assuming no texture in the grain orientation in the sample. The distribution in terms of the variable  $\delta, f(\delta)$ , is then given by

$$f(\delta) \cdot d\delta = t_1^{-1} \cdot dt \quad (\text{A5})$$

or

$$f(\delta) = (t_1 d\delta/dt)^{-1} \quad (\text{A6})$$

Inserting the derivative,  $d\delta/dt$ , from Eq. (A2a) in terms of the variable  $\delta$  and its extremal value  $\delta_1$  one finds

$$f(\delta) = \begin{cases} (2\sqrt{\delta\delta_1})^{-1} & \text{for } 0 < \delta < \delta_1 \\ 0 & \text{for all other } \delta \end{cases} \quad (\text{A7})$$

Finally we shall consider the folding of  $f(\delta)$  with the resolution function which we assume to be Gaussian,  $G(\delta)$ , with a certain standard deviation  $\sigma$ . The general expression for the observed line-shape at a spectrometer misset  $\delta_0$  from the ideal Bragg angle of  $2\theta$  is

$$I(\delta_0) = \int_{\delta=-\infty}^{\infty} G(\delta - \delta_0) f(\delta) d\delta \quad (\text{A8})$$

It is convenient to measure  $\delta$ ,  $\delta_0$  and  $\delta_1$  in units of the standard deviation  $\sigma$  so in terms of the dimensionless variables

$$x \equiv \delta/\sigma \quad , \quad x_0 \equiv \delta_0/\sigma \quad \text{and} \quad x_1 \equiv \delta_1/\sigma \quad (\text{A9})$$

we get

$$I(x_0) = \int_0^{x_1} \frac{1}{2\sqrt{xx_1}} \frac{1}{\sqrt{2\pi}} e^{-x^2/2} dx \quad (\text{A10})$$

An example is given in Fig. 13. Here the Bragg scattering angle  $2\theta_B = 10^\circ$ , and an appreciable amount of the Debye-Scherrer cone intensity ( $-28^\circ < t < 28^\circ$ ) is picked up by the 10 cm high detector at a distance of 60 cm from the sample. The corresponding maximal horizontal deviation  $\delta_1$  is  $1.2^\circ$  and the powder line has in accordance a low-angle tail extending out to  $\delta_1$ . Note that the problem is symmetric around  $2\theta = 90^\circ$ ; in other words a similar line shape, but mirrored so low angles become high angles, would occur at  $2\theta = 170^\circ$ . In practice though, the resolution which we at  $10^\circ$  take to be  $\sqrt{2}$  times the angular width of each Soller collimator, is wider at  $2\theta = 170^\circ$  due to the wavelength spread of the incident beam.

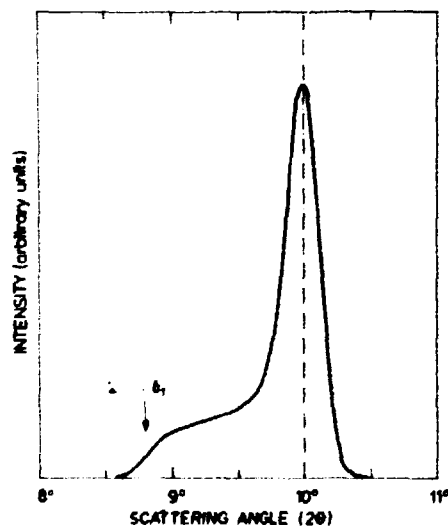


*Fig. 13. Calculated diffraction line-profile for a 10 cm high detector at  $2\theta_B = 10^\circ$ . Distance detector-sample 60 cm, collimation  $10'$  (single Soller FWHM).*

## Appendix A.4. Example of Computer Aided Line-Up Sequence

Below is an example of lining-up the spectrometer using the LU1-LU5 commands of the TASCOM system for the multidetector spectrometer. All input typed by the user has been underlined.

LU1

```

YOU ARE NOW IN LU1
PURPOSE : LINE UP MONOCHROMATOR ROTATION AND TILT

SET MONITOR COLLIMATOR TO OPEN
CHECK THAT CHANGE FROM MONOCHROMATOR TO 10 MM COLL. IS COMPLETELY OPEN
MONOCHROMATOR MOTOR DRIVE :
(1) POWER ON
(2) LINEUP ROTATION
CHECK MONITOR SCAN TO PARAMETERS
CHECK MONITOR ESCAPE INPUT TO MON COLLIMATOR
SET BEAM
TUNE MONOCHROMATOR TO DESIRED REFLECTION (ROTATION AND HEIGHT)
CHECK OFF MONOCHROMATOR MOTOR DRIVE
    
```

REFLECTION	WAVELENGTH	ROTATION POSITIVE TURNS/SEC	COUNT RATE/SEC MINIMUM
1231	4.85134	0	7.5
1111	1.42363	23	20.0
1221	7.02276	37	0.6
1402	5.44166	-3	20.0
1227	0.95402	47	4.5
1151	3.46348	53	17.0
1228	4.42304	59	5.0
1122	5.77440	63	16.0
1107	7.93134	67	7.0
1411	4.34244	70	20.0

```

IF THERE IS ANY DOUBT ABOUT THE ACTUAL MONOCHROMATOR REFLECTION
IT IS STRONGLY RECOMMENDED TO CHECK AN ALZOO REFLECTION BRIEFLY
    
```

WHEN DONE PRESS LTR. BUTTON ON CONTROL MODULE

```

YOU ARE NOW IN LU2.TAG
PURPOSE : LINEUP INCIDENT BEAM TO MON. COLLIMATOR
    
```

```

MOVE MONITOR TO AFTER 10 MM. INPUT COLLIMATOR
SET COLLIMATOR TURN TABLE TO XXXXX
CHECK TRANSLATIONS BELOW COLLIMATOR TURN TABLE ARE CENTERED
TURN ON BEAM
WHEN DONE PRESS LTR. BUTTON ON CONTROL MODULE
    
```

--- MOTOR CALIBRATION ---

```

OLD POSITIONS :
M1 = -8563.00  M2 = 0.000000  M3 = -30.0000  M4 = -28535.0  M5 = 1203.00  M6 = 20000.0  M7 = 0.000000
    
```

```

NEW POSITIONS :
M1 = -8563.00  M2 = 0.000000  M3 = 0.000000  M4 = -28535.0  M5 = 1203.00  M6 = 20000.0  M7 = 0.000000
    
```

```

SETUP CHANNELS TO PRESET TIME
WHEN DONE PRESS LTR. BUTTON ON CONTROL MODULE
PRESSING ON TO SCAN OF NO 21 POINTS , 1 SEC/POINT
    
```

24-10-78 15:27:13 FILE NAME : LU002.MLT

049111 BY 25.72 ALZOO STANDARD

```

TMR1 = 1.00249  EF = 15.2173  WF = 2.70990  LF = 2.21860  CHAN = 1.00000
EEN1 = 2.60000
    
```

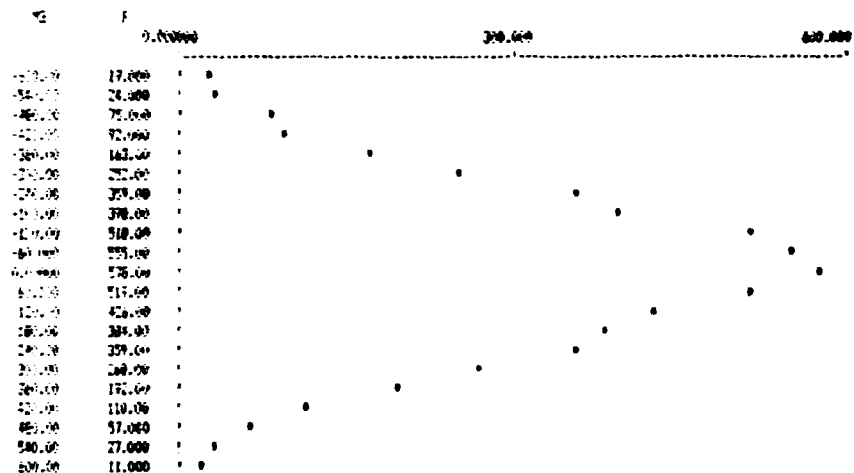
J	M1	M2	M3	M4	D	J	F	D	M0
1	-8563.	0.	1203.	20000.	0.5673	0.00000	19.000	101.00	-609.
2	-8563.	0.	1203.	20000.	0.5673	0.00000	24.000	101.00	-580.
3	-8563.	0.	1203.	20000.	0.5673	1.0000	75.000	101.00	-480.



4	-8563.	0.	1203.	2000.	0.5073	0.0000	72.00	101.00	-120.
5	-8563.	0.	1203.	2000.	0.5073	2.0000	162.00	101.00	-200.
6	-8563.	0.	1203.	2000.	0.5073	1.0000	252.00	101.00	-300.
7	-8563.	0.	1203.	2000.	0.5073	0.0000	378.00	101.00	-200.
8	-8563.	0.	1203.	2000.	0.5073	0.0000	504.00	101.00	-100.
9	-8563.	0.	1203.	2000.	0.5073	0.0000	518.00	101.00	-120.
10	-8563.	0.	1203.	2000.	0.5073	1.0000	555.00	101.00	-00.
11	-8563.	0.	1203.	2000.	0.5073	0.0000	578.00	101.00	0.
12	-8563.	0.	1203.	2000.	0.5073	1.0000	519.00	101.00	00.
13	-8563.	0.	1203.	2000.	0.5073	1.0000	420.00	101.00	120.
14	-8563.	0.	1203.	2000.	0.5073	0.0000	380.00	101.00	100.
15	-8563.	0.	1203.	2000.	0.5073	1.0000	359.00	101.00	200.
16	-8563.	0.	1203.	2000.	0.5073	1.0000	260.00	101.00	300.
17	-8563.	0.	1203.	2000.	0.5073	1.0000	172.00	101.00	300.
18	-8563.	0.	1203.	2000.	0.5073	0.0000	110.00	101.00	420.
19	-8563.	0.	1203.	2000.	0.5073	0.0000	57.000	101.00	400.
20	-8563.	0.	1203.	2000.	0.5073	1.0000	27.000	101.00	500.
21	-8563.	0.	1203.	2000.	0.5073	1.0000	11.000	101.00	600.

24-NOV-66 15:27:11 FILE NAME : L2002.DAT

SETUP AT 85.72 ALICE STANDARD



Y-MEAN : 570.000 CENTER OF MASSES : -0.000000  
 X-MEAN : 265.446 TOTAL Y : 5306.00

VARIABLE MEAN VALUE STANDARD DEVIATION  
 X 0.571029 0.597810  
 Y 250.476 170.457

AT 85.511152-RPM PER IS 2000C/S, 600 STEP FIRM  
 IF CENTER DETERMINATION IS IN PRESS LHM  
 IF CENTER DETERMINATION IS NOT IN THEN DO THE FOLLOWING:

PRESS CTRL-C, SET HD TO 000000 CENTER AND TYPE LHM

--- MOTOR CALIBRATION ---

OLD POSITIONS :  
 M1 = -8563.00 M2 = 0.000000 M3 = -1.00000 M4 = -20225.0 M5 = 1203.00 M6 = 2000.0 M7 = 0.00000

NEW POSITIONS :  
 M1 = -8563.00 M2 = 0.000000 M3 = 0.000000 M4 = -20225.0 M5 = 1203.00 M6 = 2000.0 M7 = 0.00000

YOU ARE NOW IN LHM  
 PURPOSE : ALICE SAMPLE AXIS IN BEAM

SET LHM BEAM PERFORM STANDARD ON SAMPLE POSITION  
 REMOVE SHIELDING ON SAMPLE TABLE TO PROVIDE FREE ACCESS FOR INCIDENT BEAM  
 SET REACTOR COLLIMATION TO OPEN  
 CLOSE BEAM  
 ALIGN MANUALLY DETECTOR SHIELD (M5) AND MULTICOLLIMATOR TABLE (M6)  
 WHEN CORE PAGES LHM, BUTTON ON CORE MODULE

--- MOTOR CALIBRATION ---

OLD POSITIONS :  
 M1 = -8563.00 M2 = 0.000000 M3 = 0.000000 M4 = -20225.0 M5 = 1203.00 M6 = 2000.0 M7 = 0.00000

NO PRESSURE :  
 T = 1.000000 AC = 0.000000 AD = 0.000000 AE = -0.000000 AF = 1.000000 AG = 0.000000

FOR DISPLAY PRESSURE READ FOR NO. 2000, IN PRESSURE'S SECONDARY  
 AND SOME PRESSURE IN. DURING ON LINE MODE

DATE = 08/08/00 FILE NAME = 1.000000.DAT

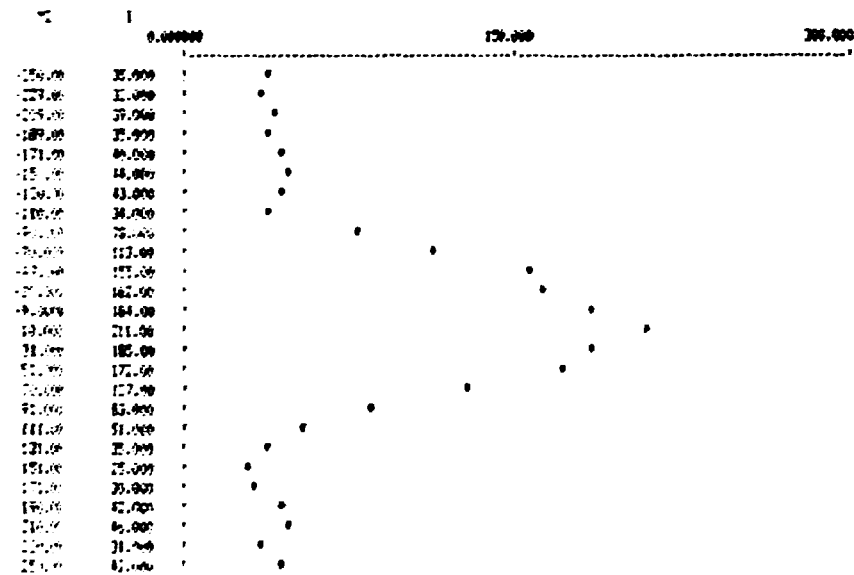
TEXT AT 05.72 (0.00) STORING

TIME = 1.000000 OF = 15.7171 MF = 2.000000 LF = 2.000000 CURR = 1.000000  
 SIZE = 1.000000

I	M	M2	M3	M4	S	F	S
1	-0.001	-2.00	2000	0.0000	0.1504	35.000	2894.0
2	-0.001	-2.00	2000	0.0000	0.1428	35.000	2799.0
3	-0.001	-2.00	2000	0.0000	0.1352	35.000	2704.0
4	-0.001	-2.00	2000	0.0000	0.1276	35.000	2609.0
5	-0.001	-2.00	2000	0.0000	0.1200	35.000	2514.0
6	-0.001	-2.00	2000	0.0000	0.1124	35.000	2419.0
7	-0.001	-2.00	2000	0.0000	0.1048	35.000	2324.0
8	-0.001	-2.00	2000	0.0000	0.0972	35.000	2229.0
9	-0.001	-2.00	2000	0.0000	0.0896	35.000	2134.0
10	-0.001	-2.00	2000	0.0000	0.0820	35.000	2039.0
11	-0.001	-2.00	2000	0.0000	0.0744	35.000	1944.0
12	-0.001	-2.00	2000	0.0000	0.0668	35.000	1849.0
13	-0.001	-2.00	2000	0.0000	0.0592	35.000	1754.0
14	-0.001	-2.00	2000	0.0000	0.0516	35.000	1659.0
15	-0.001	-2.00	2000	0.0000	0.0440	35.000	1564.0
16	-0.001	-2.00	2000	0.0000	0.0364	35.000	1469.0
17	-0.001	-2.00	2000	0.0000	0.0288	35.000	1374.0
18	-0.001	-2.00	2000	0.0000	0.0212	35.000	1279.0
19	-0.001	-2.00	2000	0.0000	0.0136	35.000	1184.0
20	-0.001	-2.00	2000	0.0000	0.0060	35.000	1089.0

DATE = 08/08/00 FILE NAME = 1.000000.DAT

TEXT AT 05.72 (0.00) STORING



TIME = 1.000000 CENTER OF MASS = 2.250000  
 SIZE = 1.000000 TOTAL Y = 2000.00

TABLE NEW VALUE STANDARD DEVIATION  
 I 15.7171 80.7870  
 F 2775.85 54.1996  
 CENTER OF MASS IS AT PRESSURE  
 CENTER OF MASS IS PROBABLY TO CENTER AND PRESSURE

NEW YORK PRESS CO. BUTTON ON CARTRIDGE

--- REVER CALIBRATION ---

NO POSITIONING :  
 X1 = -2762.0 X2 = 2.0000 X3 = 0.00000 X4 = -2772.0 X5 = 2000.0 X6 = 4490.0 X7 = 0.00000

NO POSITIONING :  
 X1 = -2762.0 X2 = 0.00000 X3 = 0.00000 X4 = -2772.0 X5 = 2000.0 X6 = 4490.0 X7 = 0.00000

AT 00:04:05(11) PRESS ON C/TS IND LEVEL=25000, JUDGE=10

NO PRESS ON C/TS

MESSAGE : FOUR ZERO FOR 2-DIGIT OF CHANNEL : AND ALIGNMENT OF X5 AND X6

WAS SCAN INTO AGAIN FROM DIRECT FROM  
 POINT 0-CLASS ATTACHED AFTER RESTART  
 REMOTE POSSIBLE SAMPLE  
 NEW YORK PRESS CO. BUTTON ON CARTRIDGE  
 READY TO SCAN TO AND TO SIMULTANEOUSLY, 17 STEPS, 2 SEC/POINT

00:04:05 15:50:47 FILE NAME : L10005.ACT

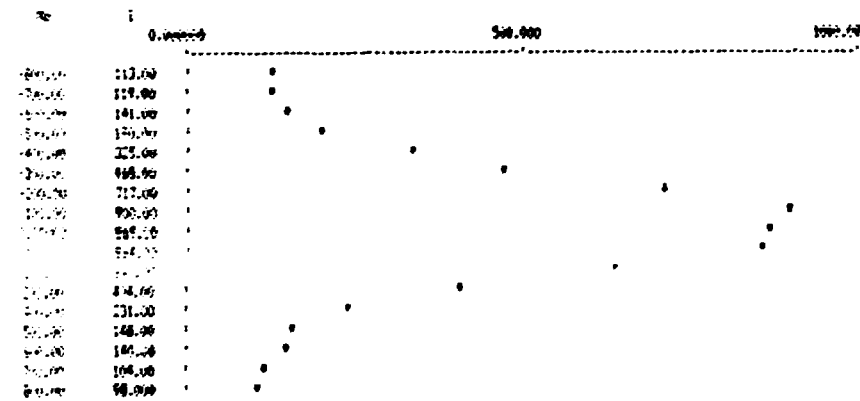
RESULTS AT 00:04:05(11) STANDARD

TIME : 00:04:05 SF : 15.2173 AF : 2.70790 CF : 2.30602 DWD : 1.00000  
 SCL : 0.00000

X	Y1	Y2	Y3	Y4	Y5	Y6	Y7	Y8
1	-2762.0	1.	-25.	-500.	0.0150	113.00	1443.0	201.00
2	-2762.0	1.	-25.	-700.	0.0146	119.00	1421.0	201.00
3	-2762.0	1.	-25.	-400.	0.0143	121.00	1526.0	201.00
4	-2762.0	1.	-25.	-500.	0.0119	129.00	1492.0	201.00
5	-2762.0	1.	-25.	-400.	0.0095	125.00	1523.0	201.00
6	-2762.0	1.	-18.	-300.	0.0071	148.00	1549.0	201.00
7	-2762.0	1.	-10.	-200.	0.0046	177.00	1431.0	201.00
8	-2762.0	1.	-5.	-100.	0.0028	200.00	1457.0	201.00
9	-2762.0	1.	0.	0.	0.0000	209.00	1505.0	201.00
10	-2762.0	1.	6.	100.	0.0028	200.00	1464.0	201.00
11	-2762.0	1.	16.	200.	0.0046	180.00	1500.0	201.00
12	-2762.0	1.	15.	300.	0.0070	164.00	1487.0	201.00
13	-2762.0	1.	20.	400.	0.0095	121.00	1523.0	201.00
14	-2762.0	1.	20.	500.	0.0119	108.00	1429.0	201.00
15	-2762.0	1.	20.	600.	0.0143	100.00	1481.0	201.00
16	-2762.0	1.	25.	700.	0.0146	104.00	1441.0	201.00
17	-2762.0	1.	40.	800.	0.0150	98.000	1404.0	201.00

00:04:05 15:50:45 FILE NAME : L10005.ACT

RESULTS AT 00:04:05(11) STANDARD



TIME : 00:04:05 CENTER OF PRESS : -10.5200  
 TIME : 00:04:05 TOTAL Y : 0471.00

VARIABLE MEAN VALUE STANDARD DEVIATION  
 X : 200.647 201.000  
 Y : 1461.25 42.5705

IF CENTER DETERMINATION IS ON PRESS LIP  
 IF CENTER DETERMINATION IS NOT ON DO  
 PRESS CTRL-C, SCAN ON TANGENT UNTIL CENTER IS FOUND

FORM 15 AND 16 TO 1980, AND BOND TO LUP

--- REFER CALIBRATION ---

DEF POSITIONS :  
 M1 = -9563.00 M2 = 1.00000 M3 = 0.00000 M4 = -2779.0 M5 = -1.00000 M6 = -16.0000 M7 = 0.00000

MEAN POSITIONS :  
 M1 = -9563.00 M2 = 1.00000 M3 = 0.00000 M4 = -2779.0 M5 = 0.00000 M6 = -16.0000 M7 = 0.00000

--- REFER CALIBRATION ---

DEF POSITIONS :  
 M1 = -9563.00 M2 = 1.00000 M3 = 0.00000 M4 = -2779.0 M5 = 0.00000 M6 = -16.0000 M7 = 0.00000

MEAN POSITIONS :  
 M1 = -9563.00 M2 = 1.00000 M3 = 0.00000 M4 = -2779.0 M5 = 0.00000 M6 = 0.00000 M7 = 0.00000

THE FOLLOWING WILL NOW CHECK THAT DETECTOR AND COLLIMATOR ARE ALIGNED  
 BY SCANNING DETECTOR BANK THROUGH COLLIMATOR BANK

24-Nov-88 16:04:22 FILE NAME : 170046.JLT

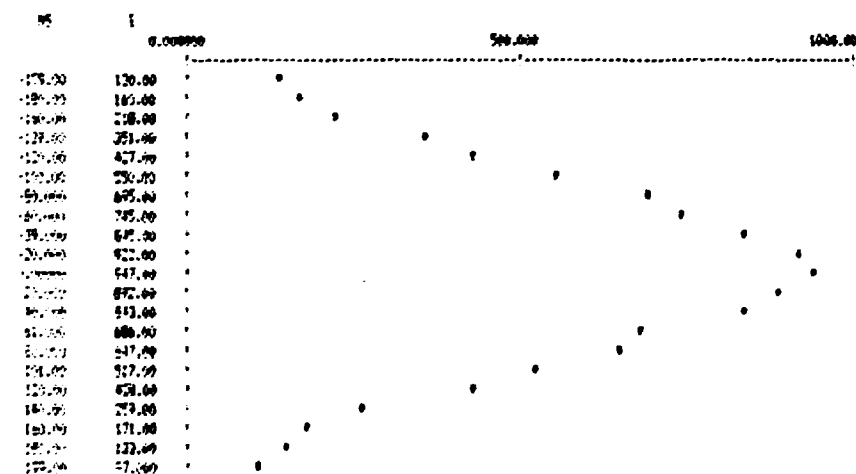
SCANNING AT 95.7% ALICE STANDBY

TOTL = 2.66340 EF = 13.2120 BF = 2.70970 LF = 2.30850 CORR = 1.46659  
 SEGM = 0.00000

I	M1	M2	M3	M4	G	I	F	B
1	-9563.	1.	-199.	0.	0.0094	120.00	1065.0	204.00
2	-9563.	1.	-180.	0.	0.0085	160.00	1542.0	204.00
3	-9563.	1.	-150.	0.	0.0076	210.00	1175.0	204.00
4	-9563.	1.	-120.	0.	0.0066	261.00	1036.0	204.00
5	-9563.	1.	-120.	0.	0.0057	327.00	1531.0	204.00
6	-9563.	1.	-100.	0.	0.0047	390.00	1470.0	204.00
7	-9563.	1.	-80.	0.	0.0038	475.00	1946.0	204.00
8	-9563.	1.	-60.	0.	0.0028	570.00	1972.0	204.00
9	-9563.	1.	-30.	0.	0.0018	685.00	1663.0	204.00
10	-9563.	1.	-20.	0.	0.0009	822.00	1663.0	204.00
11	-9563.	1.	0.	0.	0.0000	947.00	1663.0	204.00
12	-9563.	1.	20.	0.	0.0009	872.00	1620.0	204.00
13	-9563.	1.	40.	0.	0.0019	803.00	1671.0	204.00
14	-9563.	1.	61.	0.	0.0027	680.00	1685.0	204.00
15	-9563.	1.	80.	0.	0.0033	597.00	1650.0	204.00
16	-9563.	1.	101.	0.	0.0040	517.00	1530.0	204.00
17	-9563.	1.	120.	0.	0.0052	428.00	1492.0	204.00
18	-9563.	1.	140.	0.	0.0066	299.00	1477.0	204.00
19	-9563.	1.	160.	0.	0.0076	171.00	1507.0	204.00
20	-9563.	1.	180.	0.	0.0085	123.00	1657.0	204.00
21	-9563.	1.	199.	0.	0.0094	67.000	1657.0	204.00

24-Nov-88 16:04:19 FILE NAME : 170046.BAT

SCANNING AT 95.7% ALICE STANDBY



Y-MEAN : 547.000 CENTER OF MASS : -3.01374  
 Y-RMS : 222.726 TOTAL Y : 10663.0

VARIABLE MEAN VALUE STANDARD DEVIATION  
 1 507.762 295.987  
 2 1967.57 42.4762

--- MOTOR CALIBRATION ---

2LE POSITIONS :  
 M1 = -9563.00 M2 = 1.00000 M3 = 0.00000 M4 = -29752.0 M5 = -3.00000 M6 = 0.00000 M7 = 0.00000  
 NEW POSITIONS :  
 M1 = -9563.00 M2 = 1.00000 M3 = 0.00000 M4 = -29752.0 M5 = 0.00000 M6 = 0.00000 M7 = 0.00000

NOTE THE PHYSICAL ZERO ANGLE OF M6 AND NOTE IT FOR FUTURE REFERENCE

YOU ARE NOW IN LUS

PURPOSE = WAVELENGTH CALIBRATION BY STANDARD AL2O3 (0,1,2) REFLECTION

PUT AL2O3 STANDARD ON SINGLE POSITION  
 REMOVE 8-GLASS ATTENUATOR  
 LEAVE THE BEAM CLOSED  
 TAU= 3.68348  
 CHECK THAT TAU= 3.68348 CORRESPONDS TO THE ACTUAL HORIZONTAL REFLECTION

EE REFLECTION	TAU
(111)	1.92363
(113)	3.68348
(001)	4.44204
(102)	5.44086
(115)	5.72090
(132)	7.28376
(117)	7.93126
(337)	8.92462
(228)	9.42304
(339)	11.05643

IF TAU IS CORRECT PRESS LIR  
 IF TAU IS NOT CORRECT, CTRL-C, ENTER TAU IN TAU=, LUS AGAIN  
 CROSSING TIME 10.0000 FOR AL2O3 PUMPER PEAK (012) @ 3.0118  
 OPEN BEAM AND PRESS LIR  
 NOW SCAN THE SCATTERING ANGLE 1 DEG IN 26 STEPS COUNTING 10 SEC/POINT

24-MAY-68 16:30:02 FILE NAME : LIR07.PLT

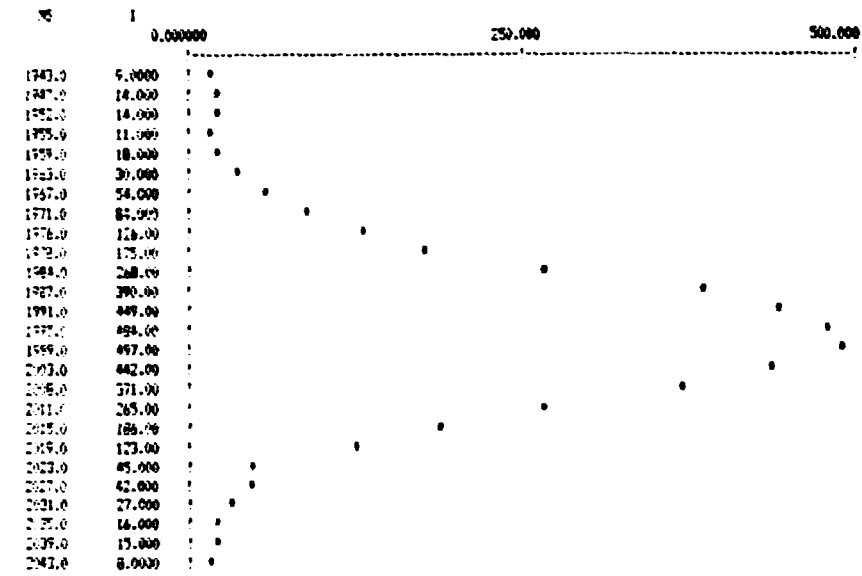
SECTION AT 05.12 AL2O3 STANDARD

TAU = 3.68348 EF = 15.2173 WF = 2.70990 LF = 2.31860 CWR = 10.0000  
 SEPR = 7.00000

J	M1	M2	M3	M4	Q	I	F	D	TTC
1	-9563.	1.	1943.	38866.	2.9931	9.0000	7536.0	1001.0	67.0290
2	-9563.	1.	1947.	38940.	2.9947	10.0000	7496.0	1001.0	67.0690
3	-9563.	1.	1952.	39020.	2.9962	10.0000	7376.0	1001.0	67.1090
4	-9563.	1.	1955.	39100.	2.9978	11.0000	7276.0	1001.0	67.1490
5	-9563.	1.	1959.	39180.	2.9994	10.0000	7228.0	1001.0	67.1890
6	-9563.	1.	1963.	39260.	3.0010	20.0000	7412.0	1001.0	67.2290
7	-9563.	1.	1967.	39340.	3.0025	50.0000	7419.0	1001.0	67.2690
8	-9563.	1.	1971.	39420.	3.0041	80.0000	7409.0	1001.0	67.3090
9	-9563.	1.	1976.	39500.	3.0057	120.0000	7556.0	1001.0	67.3490
10	-9563.	1.	1978.	39580.	3.0073	175.0000	7456.0	1001.0	67.3890
11	-9563.	1.	1984.	39660.	3.0089	240.0000	7454.0	1001.0	67.4290
12	-9563.	1.	1987.	39740.	3.0104	300.0000	7493.0	1001.0	67.4690
13	-9563.	1.	1991.	39820.	3.0120	449.0000	7334.0	1001.0	67.5090
14	-9563.	1.	1995.	39900.	3.0136	604.0000	7308.0	1001.0	67.5490
15	-9563.	1.	1999.	39980.	3.0151	697.0000	7406.0	1001.0	67.5890
16	-9563.	1.	2003.	40060.	3.0167	842.0000	7576.0	1001.0	67.6290
17	-9563.	1.	2008.	40140.	3.0183	371.0000	7314.0	1001.0	67.6690
18	-9563.	1.	2011.	40220.	3.0199	765.0000	7478.0	1001.0	67.7090
19	-9563.	1.	2015.	40300.	3.0214	186.0000	7522.0	1001.0	67.7490
20	-9563.	1.	2019.	40380.	3.0230	123.0000	7475.0	1001.0	67.7890
21	-9563.	1.	2023.	40460.	3.0246	45.0000	7429.0	1001.0	67.8290
22	-9563.	1.	2027.	40540.	3.0262	42.0000	7397.0	1001.0	67.8690
23	-9563.	1.	2031.	40620.	3.0277	27.0000	7411.0	1001.0	67.9090
24	-9563.	1.	2035.	40700.	3.0293	16.0000	7422.0	1001.0	67.9490
25	-9563.	1.	2039.	40780.	3.0309	15.0000	7346.0	1001.0	67.9890
26	-9563.	1.	2043.	40860.	3.0325	8.0000	7308.0	1001.0	68.0290

24-MAY-68 16:30:00 FILE NAME : LIR07.DAT

BE3211 AT 05.72 AL203 STANDARD



Y-MEAN : 497.000 CENTER OF MASS : 1996.43  
 Y-RMS : 27.9525 TOTAL Y : 4163.00

SINGLE MEAN VALUE STANDARD DEVIATION  
 I 169.115 173.958  
 S 7433.92 80.3199  
 IF CENTER DETERMINATION IS OK PRESS LDR  
 IF CENTER DETERMINATION IS NOT CORRECT DO

\*CAL-C, FIND PEAK IN TABLE, SET NS TO CURV AND TYPE LUS

--- MOTOR CALIBRATION ---

OLD POSITIONS :  
 M1 = -8543.00 M2 = 1.00000 M3 = 0.000000 M4 = -29752.0 M5 = 0.000000 M6 = 0.00000 M7 = 0.000000  
 NEW POSITIONS :  
 M1 = -8547.00 M2 = 1.00000 M3 = 0.000000 M4 = -29752.0 M5 = 0.000000 M6 = 0.00000 M7 = 0.000000

# Bibliographic Data Sheet

---

**Risø National Laboratory**

**Risø-M-2720**

**Title and author(s)**

The Multi-Detector Powder Neutron Diffractometer  
at Risø National Laboratory

J. Als Nielsen, N.H. Andersen, C. Broholm, K.N. Clausen and  
B. Lebech

**Date**

June 6, 1988

**Department or group**

Physics Department

**Groups own registration number(s)**

**Project/contract no.**

**Pages**

37

**Tables**

4

**Illustrations**

13

**References**

**ISBN**

87-550-1434-8

**Abstract (Max. 2000 char.)**

The report describes a new multi-detector powder neutron diffractometer installed at the DR3 reactor at Risø. The report gives details of the design criteria and operating instructions in order to ease operation of the instrument by actual and potential users. The individual components (collimators, monochromator, detectors) are described in detail. An example of a study of the oxygen uptake of  $\text{YBa}_2\text{Cu}_3\text{O}_{7-x}$  is given.

**Descriptors-INIS/EDB**

ACCURACY; COLLIMATORS; DESIGN; MONOCHROMATOR;  
NEUTRON DIFFRACTOMETERS; POWDERS; SPECIFICATIONS

**Available on request from:**

Risø Library, Risø National Laboratory, (Risø Bibliotek, Forskningscenter Risø),  
P.O. Box 49, DK-4000 Roskilde, Denmark.  
Telephone 02 37 12 12, ext. 2262. Telefax 02 36 06 09

---